Supporting Information for *Acta Phys. -Chim. Sin.* doi: 10.3866/PKU.WHXB202207007

原子尺度钴基氮碳催化剂对析氧反应的构效关系的研究

吴明亮[1]，章烨晖[1]，付战照[1]，吕之阳[2]，李强[1,*]，王金兰[1,*]

[1]东南大学物理学院，南京 211189

[2]东南大学机械工程学院，江苏省微纳生物医疗器械设计与制造重点实验室，南京 211189

Structure-Activity Relationship of Atomic-Scale Cobalt-Based N-C Catalysts in the Oxygen Evolution Reaction

Mingliang Wu [1], Yehui Zhang [1], Zhanzhao Fu [1], Zhiyang Lyu [2], Qiang Li [1,*] Jinlan Wang [1,*]

[1] School of Physics, Southeast University, Nanjing, 211189, China.

[2] Jiangsu Key Laboratory for Design and Manufacture of Micro-Nano Biomedical Instruments, School of Mechanical Engineering, Southeast University, Nanjing 211189, China.

[*]Corresponding authors. Emails: qiang.li@seu.edu.cn (Q.L.); jlwang@seu.edu.cn (J.W.).

1 Calculation method of OER activity

In the oxygen evolution reaction, the adsorption energy of the adsorbed intermediate can be defined as the equation shown below [1]:

$$\Delta E_{ads} = E_{O^*/OH^*/OOH^*} - E^* - E_{O/OH/OOH} \quad (S1)$$

For which, E^*, EO^*, EOH^* and $EOOH^*$ are the total energies of catalyst substrates, which are related to the adsorption of O, OH and OOH, respectively. The energies of O, OH, OOH and H were calculated by simulating the total energies of H_2O and H_2 molecules in the gas phase. By choosing the computational hydrogen electrode model [2], the Gibbs free energy of each adsorbate is calculated by the following expression [3]:

$$\Delta G = \Delta E_{ads} + \Delta ZPE - T\Delta S + \Delta G_U + \Delta G_{pH} \quad (S2)$$

The adsorption energy ΔE_{ads} can be calculated by DFT calculation, ΔZPE and ΔS are the changes of zero-point energy and the entropic contribution, respectively [4]. T is fixed at 289.15 K in our study. $\Delta G_U = -eU$, U denotes the applied potential. ΔG_{pH} is defined as the free energy correction of the pH, $\Delta G_{pH} = K_B T \times \ln 10 \times pH$, in which k_B is the Boltzmann constant and the pH = 0 is defined as acidic medium. The theoretical overpotential η^{OER} for electrocatalyst can be evaluated with the method in Ref. 5.

$$\eta^{OER} = \max\Delta G_1, \Delta G_2, \Delta G_3, \Delta G_4/e - 1.23\ V \quad (S3)$$

It can be inferred from the above equation that the ideal electrocatalyst requires all ΔG_i to be about 1.23 eV. More precisely, it is necessary to adjust the adsorption strength of oxygen-containing intermediates (OH*, O*, and OOH*) so that the free energy ΔG_i of each step of the reaction is in the optimal range, to ensure that the OER can spontaneously be in a position slightly higher than the equilibrium potential.

2 Polarization Curve Simulation

Following the kinetic model developed by Hansen *et al.* [6–8], we simulated the polarization curve of Co-N-C. The O electrochemical oxidation steps are listed by the following equations:

$$* + OH^- \underset{k_{-1}}{\overset{k_1}{\rightleftharpoons}} *OH + e^- \quad (S4)$$

$$*OH + OH^- \underset{k_{-2}}{\overset{k_2}{\rightleftharpoons}} *O + H_2O + e^- \quad (S5)$$

$$*O + OH^- \underset{k_{-3}}{\overset{k_3}{\rightleftharpoons}} *OOH + - e^- \quad (S6)$$

$$*OOH + OH^- \underset{k_{-4}}{\overset{k_4}{\rightleftharpoons}} O_2(aq) + H_2O + e^- \quad (S7)$$

where the adsorption sites derived from *O(aq) represent O_2 in the electrolyte. Based on the above reduction steps, we can gain the rate equations of each species, such as,

$$\frac{\partial\theta_*}{\partial t} = k_1\theta_* x_{OH^-} - k_{-1}\theta_{*OH} - k_4\theta_{*_{OOH}} x_{OH^-} + k_{-4}\theta_* x_{O_2(aq)} \quad (S9)$$

$$\frac{\partial\theta_{*OH}}{\partial t} = k_1\theta_* x_{OH^-} - k_{-1}\theta_{*OH} - k_2\theta_{*OH} x_{OH^-} + k_{-2}\theta_{*O} x_{H_2O} \quad (S10)$$

$$\frac{\partial\theta_{*O}}{\partial t} = k_2\theta_{*OH} x_{OH^-} - k_{-2}\theta_{*O} x_{H_2O} - k_3\theta_{*O} x_{OH^-} + k_{-3}\theta_{*_{OOH}} \quad (S11)$$

$$\frac{\partial\theta_{*OOH}}{\partial t} = k_3\theta_{*O} x_{OH^-} - k_{-3}\theta_{*_{OOH}} - k_4\theta_{*_{OOH}} x_{OH^-} + k_{-4}\theta_* x_{O_2(aq)} \quad (S12)$$

Here the $x_{O_2(aq)}$, x_{OH^-} and x_{H_2O} are taken as 2.34×10^{-5}, 1 and 1, respectively. θ represents the coverage of the species. These rate equations can be solved at steady state, and further infer the turnover frequency (TOF).

While for electrochemical step, K_i is associated with the reaction potential (U *vs*. RHE), given by:

$$K_i = \exp\left(-\frac{e(U - U_i)}{k_B T}\right) \quad (S13)$$

the U_i is the reversible potential at step i, which deduced by $U_i = -\Delta G_i/e$. And the k_i is written as:

$$k_i = A_i \exp\left(-\frac{E_{a,i}}{k_B T}\right) \exp\left(-\frac{e\beta_i(U - U_i)}{k_B T}\right) \quad (S14)$$

where A_i stands for effective pre-exponential factor taken as 10^9, and β_i is the symmetric factor and 0.5 is taken in this work. Since the $E_{a,i}$ of electrochemical OER steps are adopted $E_{a,I} = 0.45$ eV for all the electrochemical steps of OER on Co-N-C [9]. Moreover, the rate constants for all the reverse reaction (k_{-i}), can be deduced by:

$$k_{-i} = \frac{k_i}{K_i} \quad (S15)$$

The current density (j) can be obtained by:

$$j = e\rho \mathrm{TOF}_{e^-} \quad \text{(S16)}$$

the e is the elementary charge and ρ is the surface density of active sites and TOF_{e^-} is the turn over frequency of electrons, $e\rho = 8.368\ \mu C \cdot \mathrm{cm}^{-2}$ [10].

3 Figures and Tables

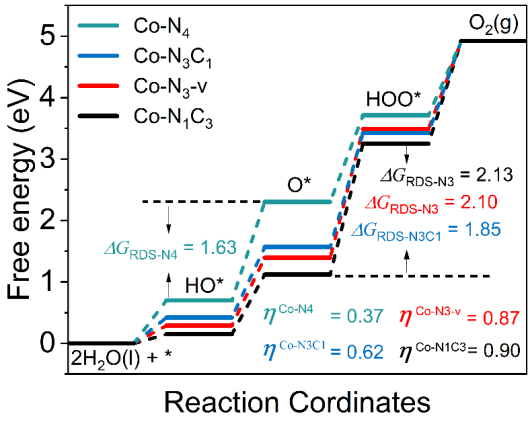

Fig. S1 Reaction energy diagram and structure models for Co-N4, CoN1C3, CoN3C1 and Co-N3-v.

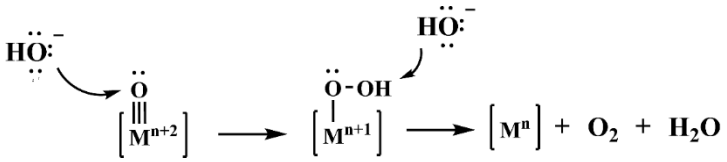

Fig. S2 Schematic illustration of possible mechanistic conversion of oxygen from metal-oxygen chains.

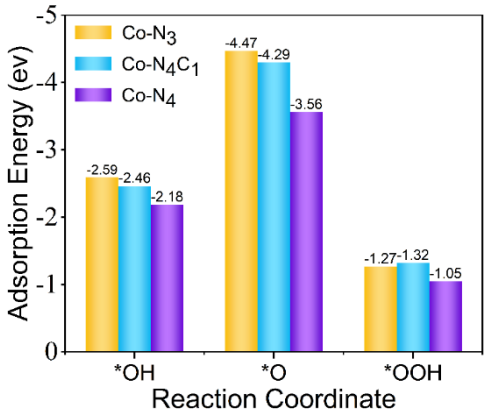

Fig. S3 Adsorption energies of oxygen-containing intermediates (*OH, *O and *OOH) on Co-N3, Co-N3C1 and Co-N4, respectively.

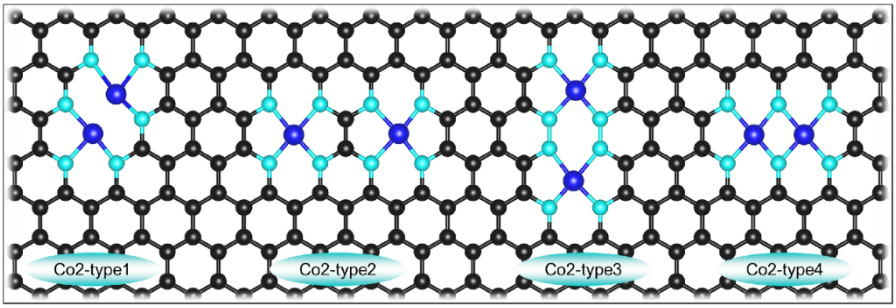

Fig. S4 Schematic diagram of the structure of diatomic Co, Co2-type1 (d_{Co-Co} = 2.33 Å), Co2-type2 (d_{Co-Co} = 4.98 Å), Co2-type3 (d_{Co-Co} = 4.08 Å), and Co2-type2 (d_{Co-Co} =2.25 Å), respectively.

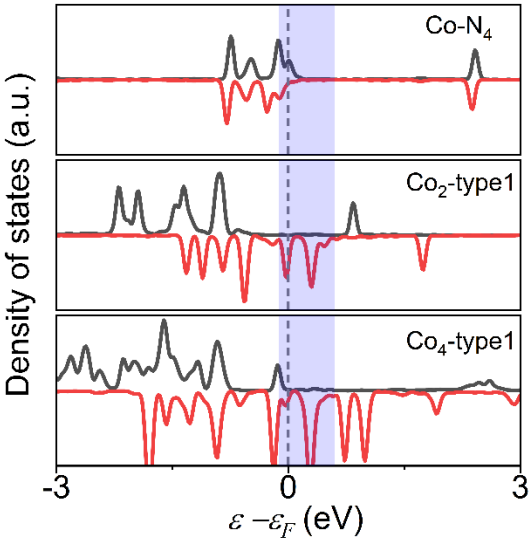

Fig. S5 The DOS of Co atom on Co-N$_4$, Co$_2$-type1 and Co$_4$-type1. The fermi energy is set to zero.

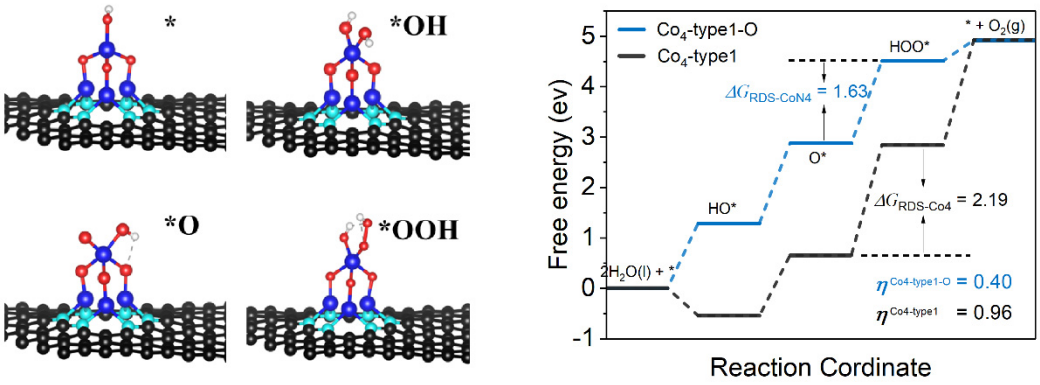

Fig. S6 The structure of O adsorbed by catalyst pre-adsorption intermediate reaction (Co$_4$-type1-O). Reaction energy diagram and structure models for Co$_4$-type1 and Co$_4$-type1-O.

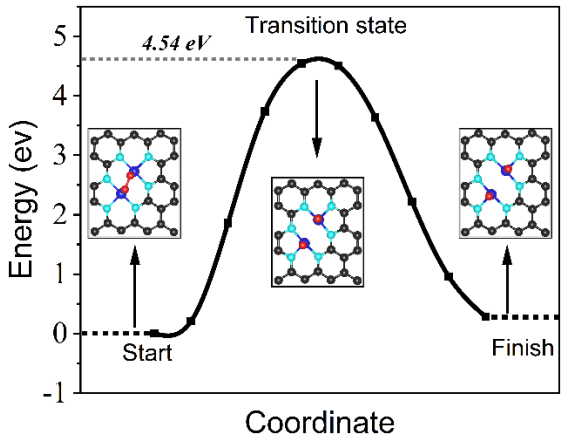

Fig. S7 Reaction pathways and transition state structures of O$_2$ dissociation at Co$_2$-type1 (It is found that O$_2$ adsorbed on Co$_2$-type1 is not easy to dissociate, and the dissociation barrier is greater than 4.5 eV through the search of the transition state).

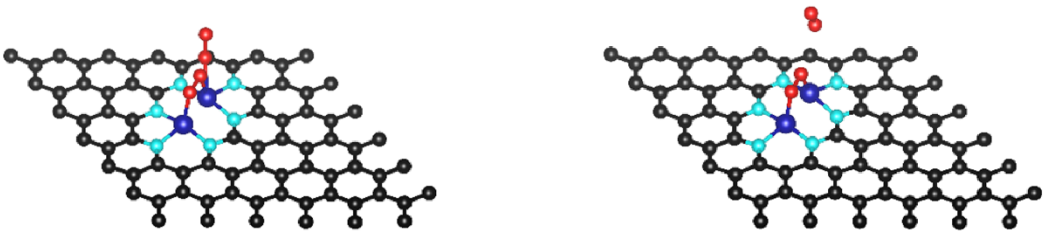

Fig. S8 The oxygen molecule adsorbs the configuration on Co_2-type1 which pre-adsorbs one oxygen molecule (One O_2 is pre-adsorbed, and the second O_2 will not be adsorbed on Co_2-type1).

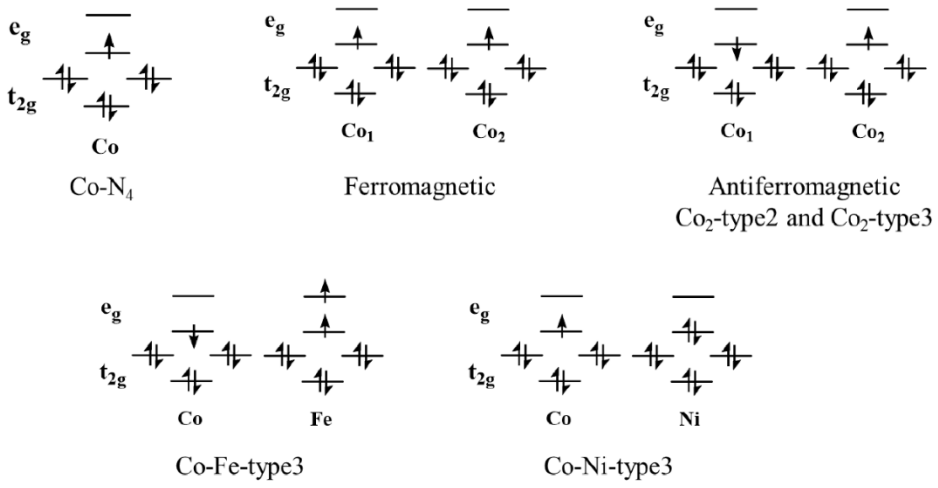

Fig. S9 Possible spin configurations of CoN_4, Co_2-type2-I, Co_2-type3-II, CoFe-type3 and CoNi-type3.

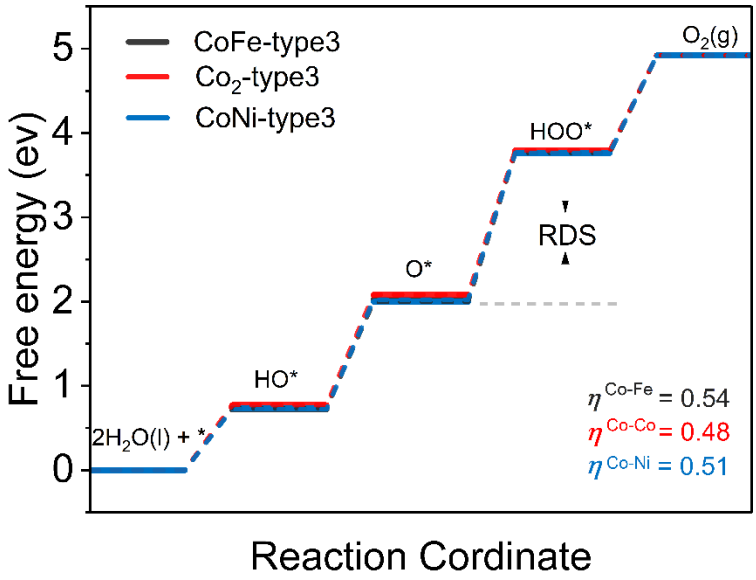

Fig. S10 Reaction energy diagram of CoFe-type3, Co_2-type3 and CoNi-type3.

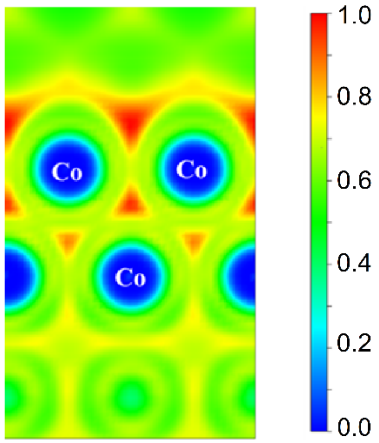

Fig. S11 The electron localization functions (ELF) contour for Co-bulk.

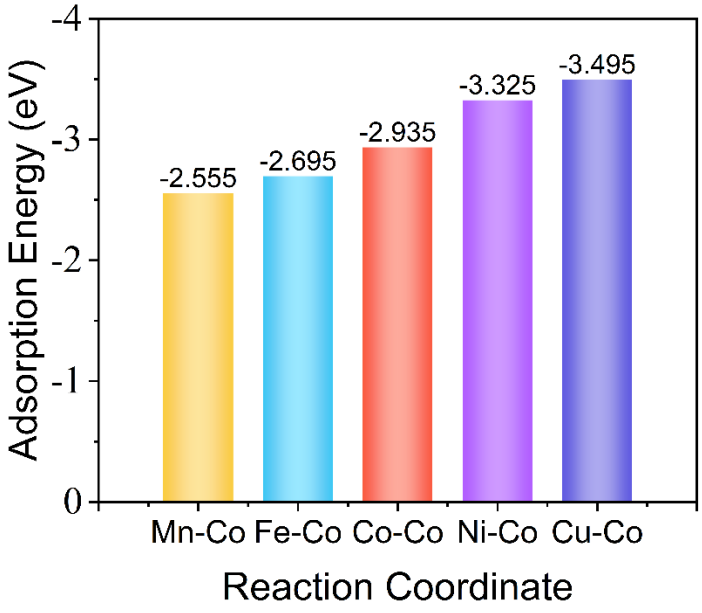

Fig. S12 Adsorption energies of O on MnCo-type4, FeCo-type4, Co_2-type4, NiCo-type4 and CuCo-type4, respectively.

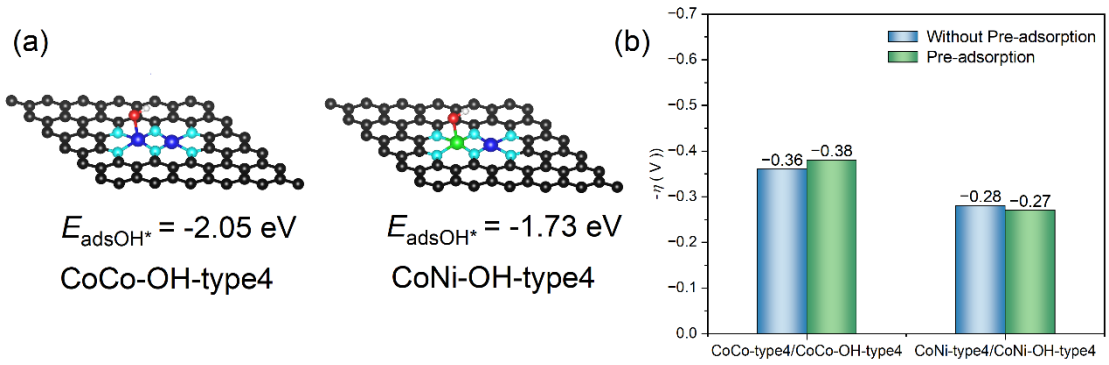

Fig. S13 (a) Structure of pre-adsorbed O* and *OH atCoCo-type4 and CoNi-type4 ortho metal sites;
(b) The change of overpotential before and after *OH pre-adsorption.

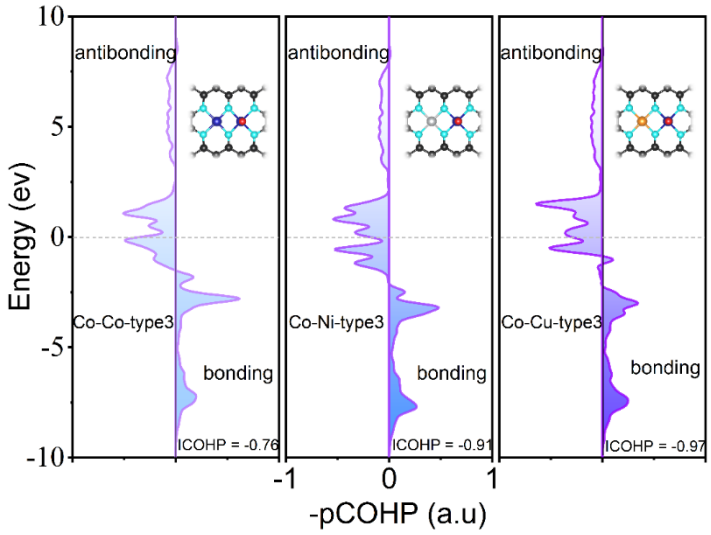

Fig. S14 COHP analysis of the Co−O bond for the adsorption of O onto Co in systems. (a) CoCo-type4, (b) CoNi-type4, and (c) CoCu-type4. −pCOHP is plotted such that negative on the graph represents the antibonding contribution and the bonding contribution is defined as positive. −ICOHP (in eV) values for different systems are given, the positive value indicates net bonding and negative antibonding. The Fermi level (E_f) is shown as a dashed gray line. Black, light blue, blue, silver and orange represent carbon, nitrogen, cobalt, nickel, and copper, respectively.

Table S1 Calculated the reaction free energy and the over-potential of OER pathway on CoN_xC_y (x = 1–4, y= 0–3).

Reaction free energy (eV) & over-potential (V)					
Configuration	ΔG_1	ΔG_2	ΔG_3	ΔG_4	η^{OER}
Co-N_1C_3 [11]	0.15	0.97	2.13	1.67	0.90
Co-N_2C_2-1	0.59	1.03	2.01	1.29	0.78
Co-N_2C_2-2	0.54	1.11	1.84	1.43	0.61
Co-N_2C_2-3	0.55	1.10	1.92	1.35	0.69
Co-N_3 [12]	0.03	2.13	1.24	1.52	0.90
Co-N_3-v	0.29	1.10	2.10	1.43	0.87
Co-N_3C_1	0.42	1.15	1.87	1.48	0.64
Co-N_4	0.70	1.60	1.41	1.21	0.37
Co-N_2C_2-2 [11]	0.53	1.07	1.86	1.45	0.63
Co-N_4 [11]	1.03	1.64	1.31	0.63	0.41
Co-N_4-exp [12]	–	–	–	–	0.38

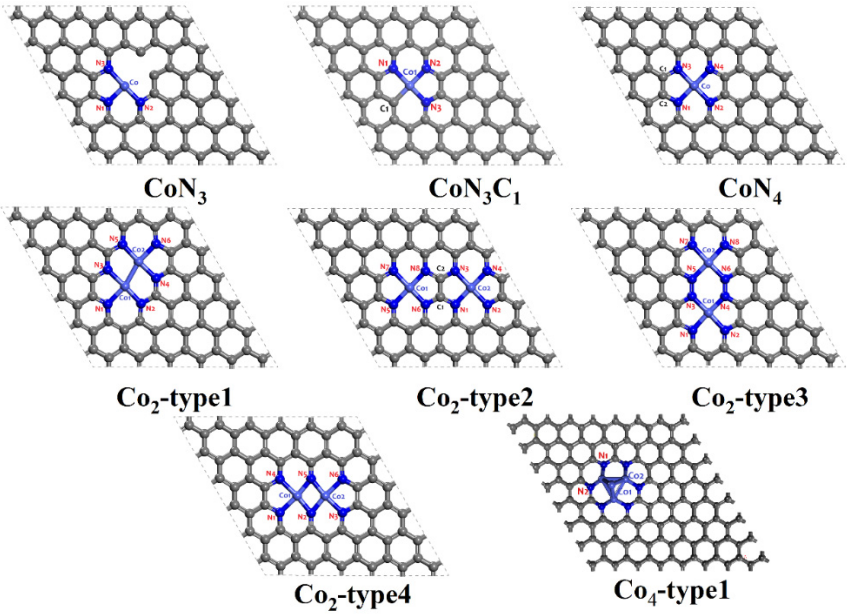

Table S2 Bader charge of the different Co-N-C system.

Bader Charge	Co1	Co2	N1	N2	N3	N4	N5	N6	N7	N8	C1	C2
CoN_3	−0.76	–	1.07	1.25	1.17	–	–	–	–	–	–	–
CoN_3C_1	−0.79		1.10	1.25	1.13	–	–	–	–	–	**0.19**	–
CoN_4	−0.89	–	1.11	1.18	1.24	1.20	–	–	–	–	**0.45**	**0.51**
Co_2-type1	−0.67	−0.67	1.17	1.13	1.17	1.25	1.14	1.13	–	–	–	–
Co_2-type2	−0.86	−0.87	1.11	1.01	1.25	1.25	1.03	1.11	–	–	–	–
Co_2-type3	−0.83	−0.83	1.15	1.141	**0.58**	**0.58**	**0.72**	**0.72**	1.15	0.15	–	–
Co_2-type4	−0.81	−0.81	1.24	1.24	1.16	1.23	1.11	1.20	1.26	1.13	**1.13**	**1.01**
Co_4-type1	−0.10	−0.50	1.22	1.20								

Table S3 The adsorption energy $E_{ads(O2)}$ (eV) of O_2 molecules adsorbed at different Co-N-C system.

System	CoN_3	CoN_3C_1	CoN_4	Co_2-type1	Co_2-type2	Co_2-type3	Co_2-type4
O_2^* adsorption energy	−1.44	−1.16	−1.23	−1.99	−1.10	−1.03	−0.43

Then, we calculated the O_2 adsorption energy of a series of Co-N-C catalysts, among which the O_2 adsorption energy of Co_2-type1 was 1.9 eV, much higher than that of Co-N_4 (−1.23 eV), Co_2-type2 (−1.1 eV), Co_2-type3 (−1.03 eV), Co_2-type4 (−0.43 eV), indicating that the adsorption energy of oxygen-containing intermediates with unsaturated coordination was generally higher, which is not conducive to oxygen evolution reaction.

Table S3 The adsorption energy $E_{ads(O2)}$ (eV) of O_2 molecules adsorbed at different Co-N-C system.

System	CoN_3	CoN_3C_1	CoN_4	Co_2-type1	Co_2-type2	Co_2-type3	Co_2-type4
O_2^* adsorption energy	−1.44	−1.16	−1.23	−1.99	−1.10	−1.03	−0.43

Then, we calculated the O_2 adsorption energy of a series of Co-N-C catalysts, among which the O_2 adsorption energy of Co_2-type1 was 1.9 eV, much higher than that of Co-N_4 (−1.23 eV), Co_2-type2 (−1.1 eV), Co_2-type3 (−1.03 eV), Co_2-type4 (−0.43 eV), indicating that the adsorption energy of oxygen-containing intermediates with unsaturated coordination was generally higher, which is not conducive to oxygen evolution reaction.

References

(1) Li, Y.; Hu, R.; Chen, Z.; Wan, X.; Shang, J.-X.; Wang, F.-H.; Shui, J. *Nano Res.* **2020,** *14*, 611. doi: 10.1007/s12274-020-3072-6

(2) Nørskov, J. K.; Rossmeisl, J.; Logadottir, A.; Lindqvist, L.; Kitchin, J. R.; Bligaard, T.; Jónsson, H. *J. Phys. Chem. B* **2004,** *108*, 17886. doi: 10.1021/jp047349j

(3) Peterson, A. A.; Abild-Pedersen, F.; Studt, F.; Rossmeisl, J.; Nørskov, J. K. *Energy Environ. Sci.* **2010,** *3*, 1311. doi: 10.1039/C0EE00071J

(4) Hu, R.; Li, Y.; Wang, F.; Shang, J. *Nanoscale* **2020,** *12*, 20413. doi: 10.1039/d0nr05202g

(5) Man, I. C.; Su, H. Y.; Calle-Vallejo, F.; Hansen, H. A.; Martínez, J. I.; Inoglu, N. G.; Kitchin, J.; Jaramillo, T. F.; Nørskov, J. K.; Rossmeisl, J. *ChemCatChem* **2011,** *3*, 1159. doi: 10.1002/cctc.201000397

(6) Hansen, H. A.; Varley, J. B.; Peterson, A. A.; Norskov, J. K. *J. Phys. Chem. Lett.* **2013,** *4*, 388. doi: 10.1021/jz3021155

(7) Hansen, H. A.; Viswanathan, V.; Nørskov, J. K. *J. Phys. Chem. C* **2014,** *118*, 6706. doi: 10.1021/jp4100608

(8) Li, Y.; Zhang, S.; Yu, J.; Wang, Q.; Sun, Q.; Jena, P. *Nano Res.* **2015,** *8*, 2901. doi: 10.1007/s12274-015-0795-x

(9) Li, L.; Yang, H.; Miao, J.; Zhang, L.; Wang, H.; Zeng, Z.; Huang, W.; Dong, X.; Liu, B. *ACS Energy Lett.* **2017,** *2*, 294. doi: 10.1021/acsenergylett.6b00681

(10) Wang, Y.; Li, Y.; Heine, T. *J. Am. Chem. Soc.* **2018,** *140*, 12732. doi: 10.1021/jacs.8b08682

(11) Sun, X.; Sun, S.; Gu, S.; Liang, Z.; Zhang, J.; Yang, Y.; Deng, Z.; Wei, P.; Peng, J.; Xu, Y.; Fang, C.; Li, Q.; Li, Han, J.; Jiang, Z.; Huang, Y. *Nano Energy* **2019,** *61*, 245. doi: 10.1016/j.nanoen.2019.04.076

(12) Zhang, Q.; Duan, Z.; Li, M.; Guan, J. *Chem. Commun.* **2020,** *56*, 794. doi: 10.1039/c9cc09007j